A Standing Wave-Type Noncontact Linear Ultrasonic Motor

Junhui Hu, *Associate Member, IEEE*, Guorong Li,
Helen Lai Wah Chan, and Chung Loong Choy

***Abstract*—In this study, a novel standing wave-type noncontact linear ultrasonic motor is proposed and analyzed. This linear ultrasonic motor uses a properly controlled ultrasonic standing wave to levitate and drive a slider. A prototype of the motor was constructed by using a wedge-shaped aluminum stator, which was placed horizontally and driven by a multilayer PZT vibrator. The levitation and motion of the slider were observed. Assuming that the driving force was generated by the turbulent acoustic streaming in the boundary air layer next to the bottom surface of the slider, a theoretical model was developed. The calculated characteristics of this motor were found to agree quite well with the experimental results. Based on the experimental and theoretical results, guidelines for increasing the displacement and speed of the slider were obtained. It was found that increasing the stator vibration displacement, or decreasing the gradient of the stator vibration velocity and the weight per unit area of the slider, led to an increase of the slider displacement. It was also found that increasing the amplitude and gradient of the stator vibration velocity, or decreasing the weight per unit area of the slider and the driving frequency, gave rise to an increase of the slider speed. There exists an optimum roughness of the bottom surface of the slider at which the slider speed has a maximum.**

I. Introduction

To broaden the range of applications of ultrasonic motors, noncontact ultrasonic motors have been proposed and studied [1]–[16]. Noncontact ultrasonic motors are a class of ultrasonic motors for which there is no direct contact between the stator and the rotor or slider. In a noncontact ultrasonic motor, there is a fluid between the stator and the rotor or slider. An ultrasonic vibration is excited in the stator, and this ultrasonic vibration excites a sound field in the fluid between the stator and the rotor. When the sound field in the fluid is controlled properly, acoustic streaming and acoustic radiation force can be induced, which drive a properly designed rotor or slider into motion. Usually, air, water, a solution, or an electro-rheologic fluid is used. When fast movement is required, air is used because it is more difficult to saturate the sound field in air than that in other fluids [16]. The rotor of a noncontact ultrasonic motor is supported by a bearing structure or levitated by the acoustic radiation force.

Compared with electromagnetic motors, noncontact ultrasonic motors have the advantages that they have simple structures and the operation is free of electromagnetic noise. Compared with contact-type ultrasonic motors, they can have higher revolution speeds and can operate continuously without wear. A noncontact ultrasonic motor with the rotor levitated by an axial acoustic viscous force has achieved a revolution speed of 4400 rpm [9], [11]. Also, a travelling wave-type noncontact linear ultrasonic motor can levitate and transport a planar object of 8.6 g at a speed of 0.7 m/s [13]–[15]. Noncontact rotary ultrasonic motors with high revolution speeds have potential applications in compact disk driving systems, choppers for sensors, and IC cooling systems. In addition, noncontact linear ultrasonic motors can be used in transportation systems for silicon wafers, IC chips, and various kinds of business cards.

In previous works, an ultrasonic travelling wave along the stator has been used to drive the slider of noncontact linear ultrasonic motors [13]–[15]. In this study, we propose a noncontact linear ultrasonic motor that uses a standing wave. A wedge-shaped stator is used for generating a gradient of the stator vibration amplitude along the length of the stator. A solid object with a planar bottom surface such as a MEMS device, a glass substrate, an IC chip, or a metal plate can be levitated and transported by this motor. A theoretical model has been developed for analyzing the operation of this motor. For unidirectional transportation, this motor has a simpler structure and is of lower cost than the traveling wave-type because only one vibrator is needed to drive the stator.

II. Construction

The construction of the motor is shown in Fig. 1 and 2. The rectangular plate-shaped stator, made of aluminum, consists of two parts: a vibration excitation part and an operation part. The vibration excitation part has uniform thickness along the length direction, and the operation part is wedged along the length direction. A multilayer PZT vibrator is bolted between the vibration excitation part and a metal support plate such that a flexural vibration is induced in the stator. The slider is an object with a planar bottom surface such as a piece of glass, metal, or silicon. The length of the wedge-shaped part is 283 mm, the

Manuscript received January 21, 2000; accepted December 6, 2000. Financial support from the Hong Kong Polytechnic University Postdoctoral Research Fellow Scheme and the Center for Smart Materials is acknowledged.

The authors are with the Center for Smart Materials and Department of Applied Physics, The Hong Kong Polytechnic University, Hung Hom, Kowloon, Hong Kong (e-mail: fjhui@hotmail.com).

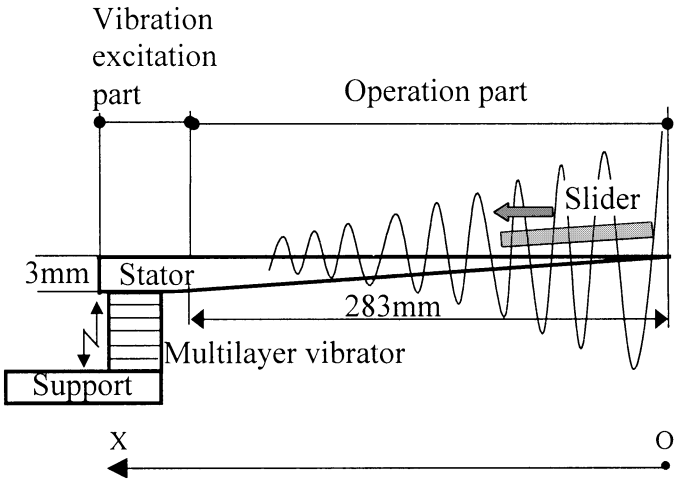

Fig. 1. Construction of a standing wave-type noncontact linear ultrasonic motor.

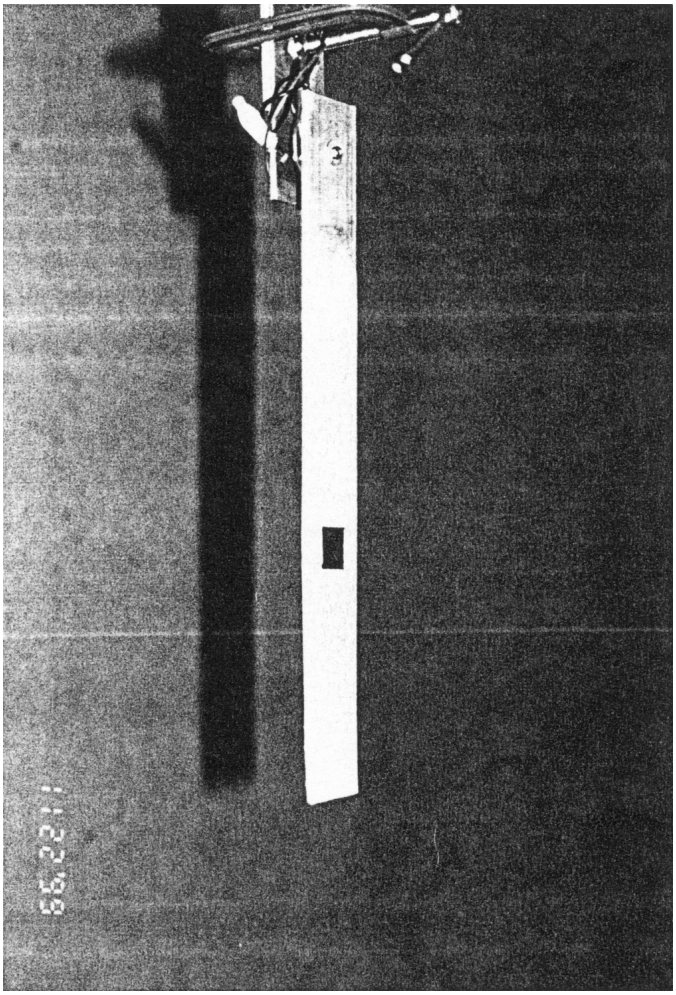

Fig. 2. Photograph of the standing wave-type noncontact linear ultrasonic motor.

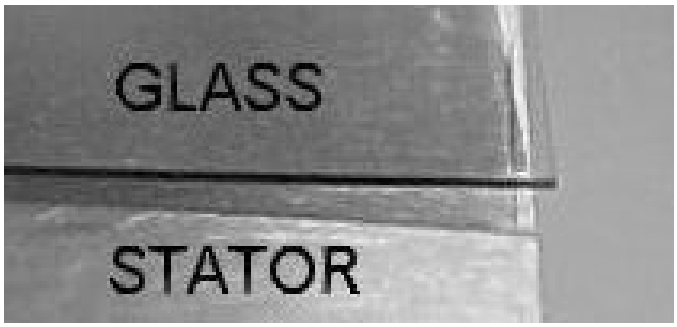

Fig. 3. Levitation of a glass slider.

thickness of the vibration excitation part is 3 mm, and the height and outer diameter of the multilayer PZT vibrator are 14 and 12.7 mm, respectively. The driving frequency of the motor is 88.8 kHz. The upper surface of the stator is accurately adjusted to lie horizontally.

When an AC voltage whose frequency equals the resonance frequency of the stator flexural vibration is applied to the PZT vibrator, the slider on the horizontal stator is levitated in the vertical direction and driven to move in the horizontal direction. The moving direction of the slider is from the tip of the stator to the vibration excitation part of the stator. To obtain sufficiently high driving force, it was experimentally found that the length of the slider should be larger than one wavelength of the stator vibration. The levitation of a glass slider of weight 1.5 mN and dimensions $20 \times 20 \times 0.15$ mm was observed by a video camera, and the levitation of the slider at the tip of the stator is shown in Fig. 3. The whole surface of the glass plate was covered with a gold film, and a beam of light shone on the glass. When the glass was levitated, a shadow was observed, as shown in Fig. 3. Using a laser Doppler vibrometer, the stator vibration velocity was measured as a function of distance x from the tip of the stator, and the result for the range 80 mm $< x <$ 0 mm is shown in Fig. 4. It is seen that the amplitude of the vibration velocity decreases with increasing x.

III. Principle of Operation

The principle of this motor can be explained by referring to Fig. 5(a and b). It is assumed that the length of the slider is larger than one wavelength of the stator vibration. When the stator is set into flexural vibration, a sound field is created between the stator and the slider. If the sound field is strong enough, the slider on the stator can be levitated vertically by the near field acoustic radiation force. Meanwhile, a turbulent acoustic streaming of air parallel to the bottom surface of the slider is generated in the boundary layer next to the bottom surface of the slider by the gradient of the stator vibration amplitude. This turbulent acoustic streaming generates an unidirectional shearing force acting on the slider surface because of the eddy viscosity of air, and this force drives the levitated slider to move in the horizontal direction. In addition, because

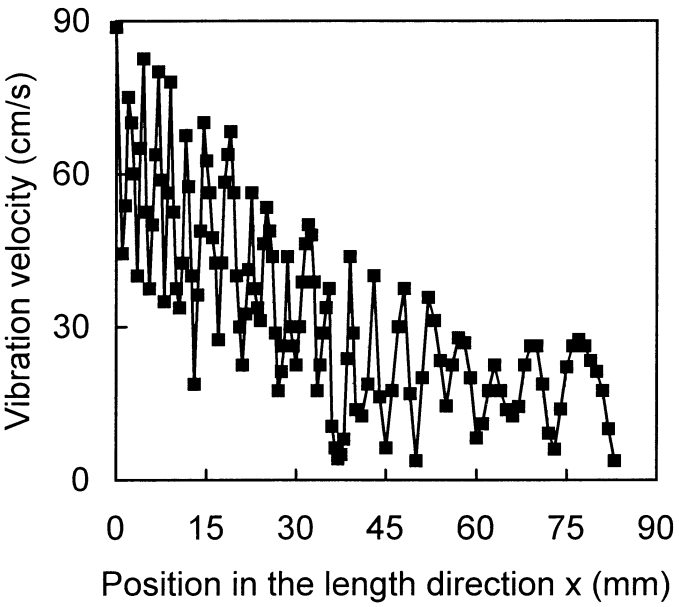

Fig. 4. Variation of the stator vibration velocity with position.

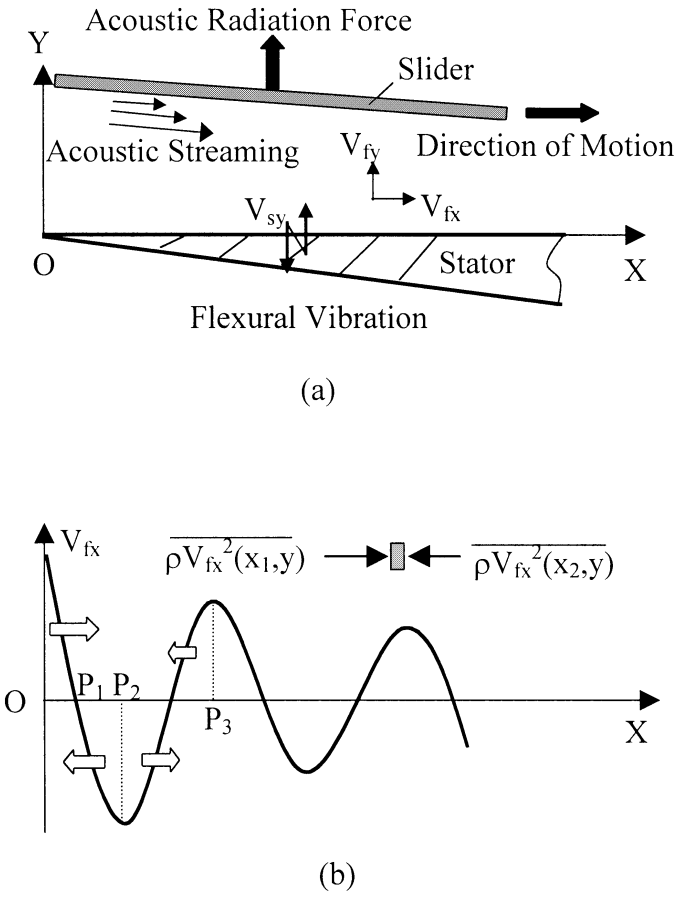

Fig. 5. Principle of the motor. a) Sound field and acoustic streaming between the stator and the slider; b) sound field distribution and normal Reynolds' stress.

of the gradient of the stator vibration amplitude, the levitation distance between the slider and the stator changes with position. The levitation distance decreases with decreasing stator vibration amplitude. When the levitation distance becomes very small, the slider stops because of the friction between the slider and the stator.

The occurrence of the acoustic streaming is explained as follows. Because the stator vibration velocity V_{sy} has a gradient in the length direction, the sound field between the stator and the slider has a horizontal component $V_{fx}(x, y)$ in addition to a vertical component $V_{fy}(x, y)$. Thus, a fluid element between the stator and the slider experiences a Reynolds' normal stress $\overline{\rho V_{fx}^2}$ as shown in Fig. 5(b), where the bar denotes averaging over time [17], [18]. Reynolds' shear stress is not given in Fig. 5(b) because a further analysis shows that it hardly contributes to the acoustic streaming. Because of Reynolds' normal stress, the air layer in the range [O, P_1] tends to flow in the +X direction, and the air layer in the range [P_1, P_2] tends to flow in the −X direction. Because the amplitude of the stator vibration decreases in the +X direction, the amplitude of air vibration velocity V_{fx} also decreases in the +X direction. So, the air flow trend in the range [O, P_1] is stronger than that in the range [P_1, P_2], and the net air flow in the range [O, P_2] (half wavelength) is in the +X direction. For the same reason, the air in the range [P_2, P_3] of another half wavelength also flows in the +X direction. Therefore, there is a unidirectional acoustic streaming on the bottom surface of the slider. Furthermore, the acoustic streaming can be regarded as a turbulent flow approximately because of the vibration and flow of air in the +Y direction.

IV. Theoretical Model

A theoretical model for this motor was developed on the basis of the preceding explanation and the experimental results. The model consists of three parts involving analysis of A) the sound field between the stator and the slider, B) the driving force acting on the slider, and C) the characteristics of the motor.

A. Sound Field Between the Stator and the Slider

For the convenience of analysis, it is assumed that the stator vibration velocity in the +Y direction V_{sy} is given by

$$V_{sy} = V_{sym}(x) \cos k_x x \cos \omega t \tag{1}$$

where ω is the angular frequency of the stator vibration, k_x is the average wave number in the operation part, and $V_{sym}(x)$ is the amplitude of the stator vibration velocity. For the prototype motor, k_x is 1624.2 rad/m, so the wavelength ($=2\pi/k_x$) is 3.87 mm. The peak values of the stator vibration velocity were measured in the range $0 < x < 300$ mm, and their asymptote is shown in Fig. 6. From this figure, it is known that $V_{sym}(x)$ can be expressed as

$$V_{sym}(x) = V_0 e^{-ax} \tag{2}$$

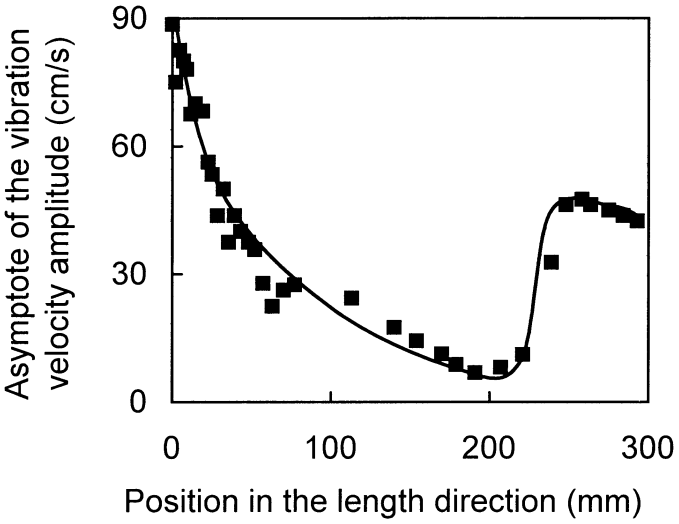

Fig. 6. Normalized asymptote of the amplitude of the stator vibration velocity.

where V_0 is the amplitude of the stator vibration velocity at $x = 0$, and a is the spatial attenuation factor of the stator vibration, which is calculated as 12 m^{-1} for the prototype motor.

In the analysis of the sound field between the stator and the slider, only the sound field that is outside the boundary layers on the surfaces of stator and slider is analyzed. The slider that has a length of L is located in the range $[x, x + L]$. The average levitation distance in this range is assumed to be roughly constant and has an average value h_a, which is a function of x. Also, it is assumed that the sound field is linear and has no vibration component in the Z direction.

The sound field is governed by the following wave equation and boundary conditions:

$$\frac{\partial^2 \varphi}{\partial^2 t} = c^2 \nabla^2 \varphi \tag{3}$$

$$\mathbf{V_f} = V_{fx} i + V_{fy} j = -\nabla \varphi \tag{4}$$

$$V_{fy}|_{y=0} = V_{sy} \qquad V_{fy}|_{y=h_a} = 0 \tag{5}$$

where c is the velocity of sound in air, φ is the potential of the vibration velocity, $\mathbf{V_f}$ is the vibration velocity of the fluid between the stator and the slider, and V_{fx} and V_{fy} are the components of $\mathbf{V_f}$ in the X and Y directions, respectively. Eq. (3) can be derived from the mass conservation equation, Euler's equation, and the pressure-density relationship [17], [22]. From (4), we have

$$V_{fx} = -\frac{\partial \varphi}{\partial x} \tag{6}$$

$$V_{fy} = -\frac{\partial \varphi}{\partial y}. \tag{7}$$

Substituting (1) and (7) into (5), the boundary conditions are transformed into

$$\frac{\partial \varphi}{\partial y}|_{y=0} = -V_{sym}(x) \cos k_x x \cos \omega t \tag{8}$$

$$\frac{\partial \varphi}{\partial y}|_{y=h_a} = 0. \tag{9}$$

From (3), (8), and (9), we have

$$\varphi = -\frac{V_{sym}(x)}{\beta} (\sin \beta y + ctg\beta h_a \cos \beta y) \cos k_x x \cos \omega t \tag{10}$$

where

$$\beta^2 = (\omega/c)^2 - k_x^2. \tag{11}$$

Substituting (10) into (6) and (7), the vibration velocities of air are given by

$$V_{fx} = V_{fxm} \cos \omega t \tag{12}$$

$$V_{fxm} = \frac{1}{\beta} (\sin \beta y + ctg\beta h_a \cos \beta y) \left[\frac{dV_{sym}(x)}{dx} \cos k_x x - k_x V_{sym}(x) \sin k_x x \right] \tag{13}$$

$$V_{fy} = (\cos \beta y - ctg\beta h_a \sin \beta y) V_{sym}(x) \cos k_x x \cos \omega t. \tag{14}$$

B. Driving Force Acting on the Slider

From (1), the amplitude of the stator vibration displacement is

$$A(x) = V_{sym}(x) \cos(k_x x)/\omega = \frac{V_0}{\omega} e^{-ax} \cos(k_x x). \tag{15}$$

For a slider of length L, width W, and weight mg located in the region $[x, x + L]$, the following relation holds [19]:

$$W \int_x^{x+L} \frac{1}{4}(1+\gamma)\rho c^2 \frac{A^2(X)}{h_a^2} dX = mg \tag{16}$$

where ρ and γ are the density and the specific heat ratio of air, respectively. Because h_a is a constant for a given x, we have

$$h_a = \frac{c}{2} \sqrt{\frac{(1+\gamma)\rho W}{mg} \int_x^{x+L} A^2(X) dX}. \tag{17}$$

Substituting (2) and (15) into (17), we obtain the approximate expression:

$$h_a = \frac{B V_0 e^{-ax}}{\omega \sqrt{mg/(LW)}} \tag{18}$$

where

$$B = \frac{1}{4} \sqrt{2(1+\gamma)\rho c^2} \sqrt{1 - aL + 2a^2 L^2/3} \sqrt{1 + a^2/(a^2 + k_x^2)}. \tag{19}$$

Further, by means of the theory of acoustic streaming in the boundary layer [16], [20], [21], the driving stress acting on the slider surface in the horizontal direction is

$$\tau_x = -0.25 \rho \delta \frac{\mu_e}{\mu} \left(\frac{\partial V_{fxm}}{\partial x} V_{fxm} \right)_{y=h_a} \tag{20}$$

where

$$\delta = \left(\frac{2\mu}{\omega\rho}\right)^{0.5} \tag{21}$$

is the thickness of the acoustic boundary layer on the bottom surface of the slider, and μ_e and μ are the eddy and shearing viscous coefficient of air, respectively. From (2), (13), and (20), the driving force acting on the slider located in the region $[x, x+L]$ is approximately

$$F(x) = 0.125\ \rho\delta\ \frac{\mu_e}{\mu}\ \frac{a^2(1-e^{-2aL})W}{\beta^2 \sin^2 \beta h_a}\ V_0^2\ e^{-2ax}. \tag{22}$$

A previous experimental study [16] indicates that the ratio μ_e/μ depends on the roughness of the bottom surface of the slider R_z (ten-point average roughness) and the turbulence of the acoustic streaming in the boundary layer on the bottom surface of the slider. The turbulence is caused mainly by the air motion in the vertical direction. The stronger this air motion, the stronger the turbulence. Moreover, this air motion becomes weaker as the distance between the stator and the slider decreases. Based on these results, we assume that

$$\frac{\mu_e}{\mu} = C_e \left(\frac{h_a}{\delta}\right)^{\xi} \tag{23}$$

where C_e is a constant. The experimental results in this study indicate that $\xi = 3$; so this value will be used in the derivation of the average slider speed u in the following section.

C. Characteristics of the Motor

The displacement of the slider from the tip of the stator to the stopping place can be obtained from [17]:

$$l = \frac{1}{a} \ln \frac{V_0 B}{\omega h_{cr} \sqrt{mg/(WL)}} \tag{24}$$

where h_{cr} is the critical levitation distance at which the slider stops. The slider speed $u(x)$ at the position $[x, x+L]$ can be approximately found by equating the driving force with the drag force:

$$F(x) = WL\frac{\rho}{2} C_d u^2(x) \tag{25}$$

where C_d is the drag coefficient. By using (18), (22), (23), (25) and the relationship $k_x >> a$ and $\beta h_a << 1$, the average slider speed u in the range $0 < x < l$ is given by

$$\begin{aligned} u =& \frac{1}{l}\int_0^l u(x)dx \\ =& C_{av} a^{1.5} \beta^{-2} B^{0.5} \delta^{-1} \omega^{-0.5} \\ & (C_e/C_d)^{0.5}\, V_0^{1.5} (mg/WL)^{-0.25} \end{aligned} \tag{26}$$

where

$$C_{av} = \frac{1 - e^{-1.5al}}{1.5\sqrt{2}al}. \tag{27}$$

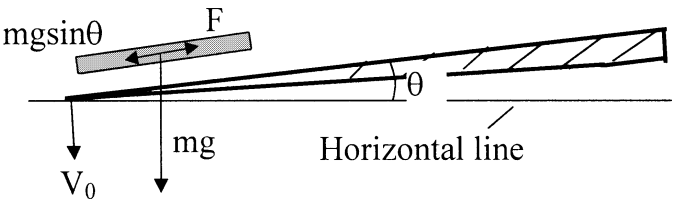

Fig. 7. Approximate measurement of the driving force.

V. Measurements

A laser Doppler vibrometer (Polytech OFV3001) was used to measure the stator vibration velocity. The upper surface of the stator was accurately adjusted to lie in a horizontal plane, and the displacement of the slider was measured. The average slider speed was calculated by dividing the slider displacement (l) from the tip of the stator to its stopping place by the time taken to make this displacement. The driving force on the slider was measured approximately by the way shown in Fig. 7. The stator was fixed at a small tilting angle θ with the horizontal plane. The slider was placed on the stator. When the slider was levitated, the angle θ was adjusted until the driving force F and the gravity component $mg\sin\theta$ balanced each other. The driving force F was then calculated from

$$F = mg\sin\theta. \tag{28}$$

Theoretically, it can be proved that the driving force obtained this way is approximately equal to the real one if θ is very small. Glass and brass sliders were used in our experiments. In addition, abrasive powder with various particle sizes was used for producing different roughness on the bottom surface of the slider.

VI. Results and Discussion

In this section, unless otherwise specified, the experiment and/or calculation were carried out under the following conditions. 1) The driving frequency f is 88.8 kHz. 2) The wave number of the stator vibration k_x is 1624.2 rad/m. 3) The spatial attenuation factor of the stator vibration a is 12 m^{-1}. 4) The glass slider is a rectangular plate, which has dimensions $20 \times 20 \times 0.15$ mm, surface roughness (R_z) of 0.2 μm, and weight per unit area of 0.37 $\mathrm{mN/cm^2}$. 5) The brass slider is a circular washer, which has an outer diameter of 11.4 mm, inner diameter of 3.6 mm, thickness of 1.0 mm, surface roughness of 5 μm, and weight per unit area of 7.4 $\mathrm{mN/cm^2}$. 6) C_e was found by comparing the measured driving force with (22). $C_e = 3.1\times10^{-3}$ and 9.1×10^{-3} for the glass and brass sliders, respectively. 7) h_{cr} was found by comparing the measured slider displacement with (24). $h_{cr} = 17$ and 6 μm for the glass and brass sliders, respectively. 8) Assuming that C_d is the same for the glass and brass sliders, $C_d = 2.9$, as found by comparing the measured slider speed with (26). Also, the properties of air used in the calculation are shown

TABLE I
PROPERTIES OF AIR USED IN THE CALCULATION.

Density ρ (kg/m^3)	1.2
Sound velocity c (m/s)	343
Specific heat ratio γ	1.4
Viscosity μ (kg/m/s)	1.81×10^{-5}

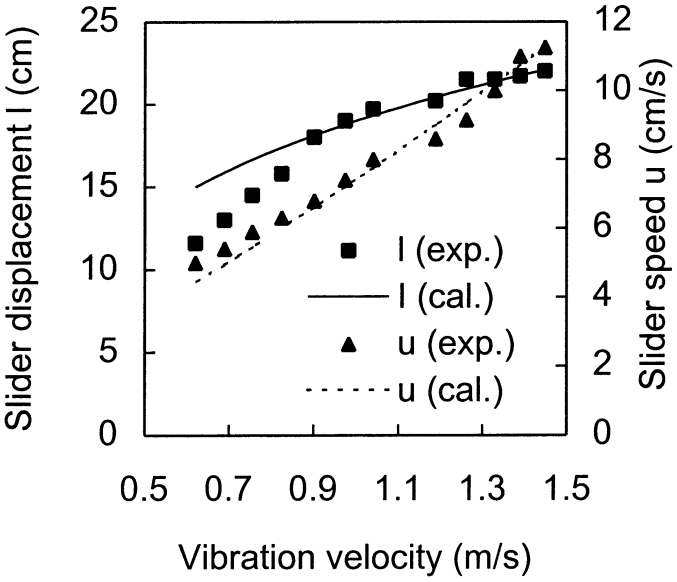

Fig. 8. Dependence of the displacement and average speed of the glass slider on the stator vibration velocity.

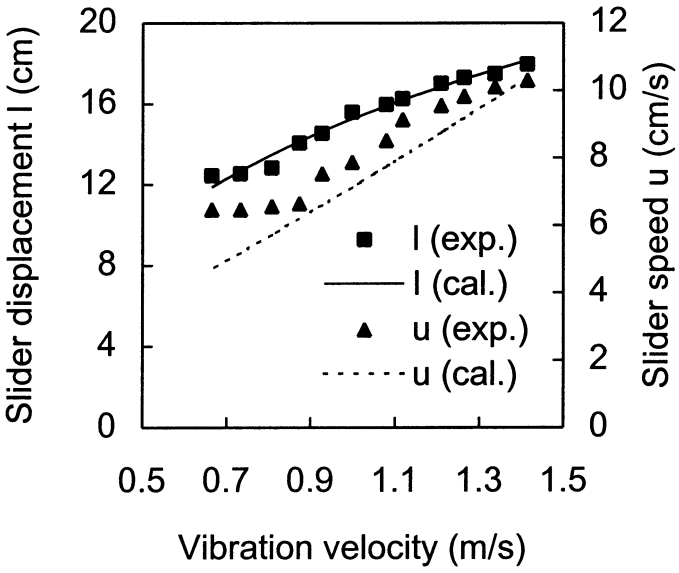

Fig. 9. Dependence of the displacement and average speed of the brass slider on the stator vibration velocity.

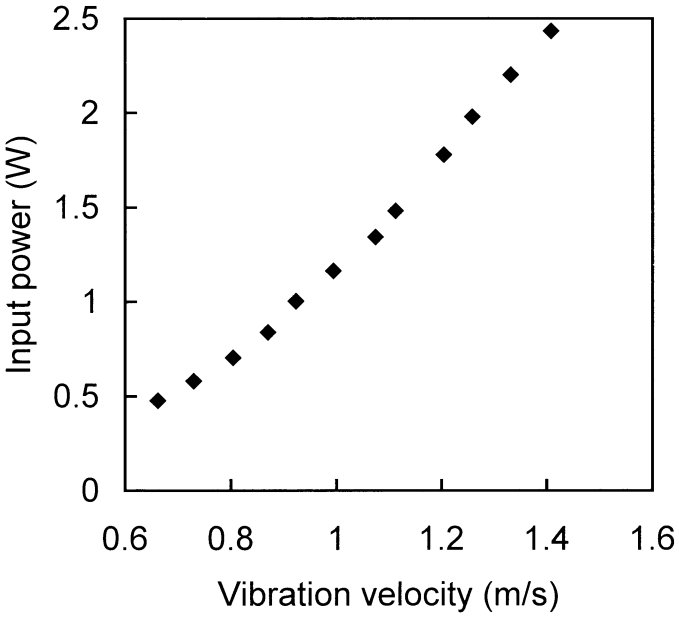

Fig. 10. Input electrical power versus stator vibration velocity for the brass slider. The points are experimental data.

in Table I. In the following figures, the slider displacement l means the displacement of the slider from the tip of the stator to the stopping place, the slider speed u means the average speed within the range $0 < x < l$, and the vibration velocity V_0 means the peak vibration velocity at the tip of the stator.

The dependencies of the slider displacement l and the average slider speed u on the stator vibration velocity V_0 are shown for the glass and brass sliders in Fig. 8 and 9, respectively. It is observed that both l and u increase with increasing V_0. The displacement and speed of the sliders were also calculated using (24) and (26), respectively, and Fig. 8 and 9 show that there is good agreement between the theoretical and experimental results.

For the brass slider, the observed relationship between the input electrical power and the stator vibration velocity V_0 is shown in Fig. 10. By comparing the data in Fig. 9 and 10, it is observed that the brass slider can be transported 17 cm at an average speed of 10 cm/s by using an input power of 2.5 W.

Fig. 11 shows a comparison between the calculated driving force acting on the glass slider and the experimental data. At $V_0 < 1$ m/s, there is good agreement between the theoretical and experimental results. The driving force increases with the stator vibration velocity. This is because the acoustic streaming between the stator and the slider increases with the stator vibration velocity. It is also found that the driving force is much less than the measured frictional force of 0.5 mN, indicating that the slider is levitated.

The dependence of the slider displacement on the weight per unit area of the brass slider was investigated experimentally and theoretically at a constant stator vibration velocity ($V_0 = 1.4$ m/s), and the results are shown in Fig. 12. It is observed that the decrease of the slider displacement with increasing weight per unit area of the slider is well reproduced by the theoretical calculation. As the weight per unit area of slider increases, the levita-

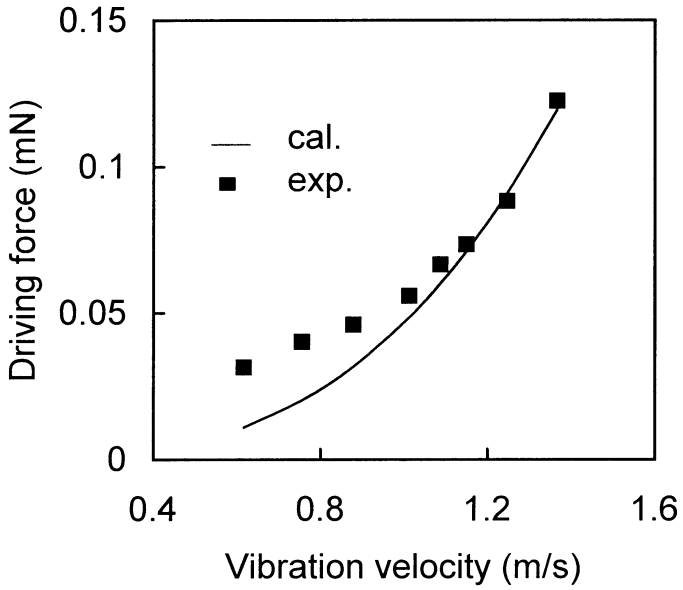

Fig. 11. Driving force versus stator vibration velocity for the glass slider.

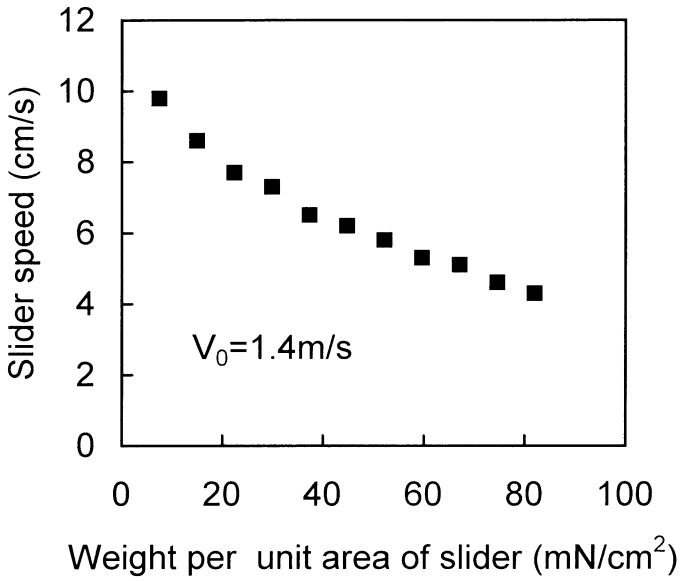

Fig. 13. Average slider speed versus weight per area of the brass slider. The points are experimental data.

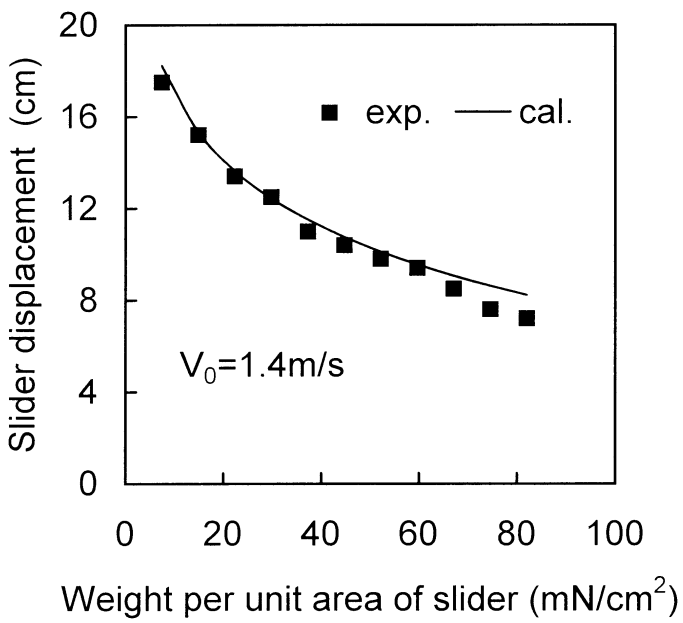

Fig. 12. Slider displacement versus weight per unit area of the brass slider.

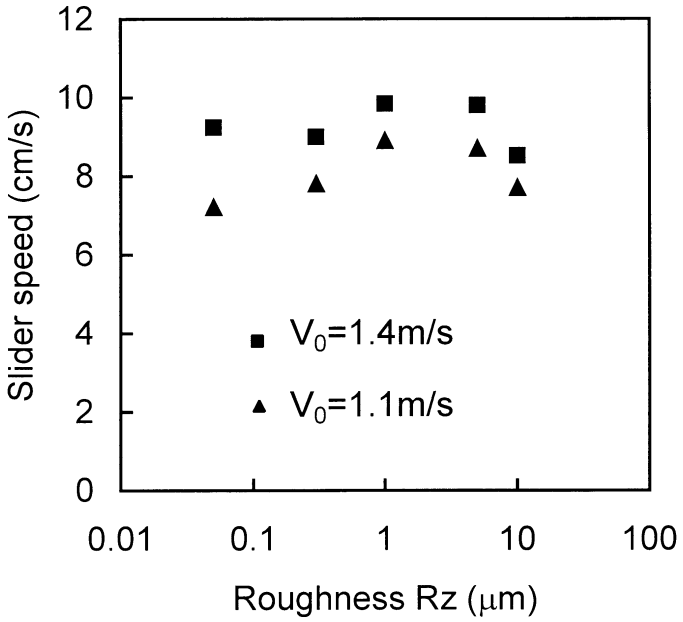

Fig. 14. Effect of the roughness of the bottom surface of the brass slider on the average slider speed. The points are experimental data.

tion distance decreases [see (18)], so the levitation distance reaches the critical value h_{cr} at a position closer to the tip of the stator.

The dependence of the average slider speed on the weight per unit area of the brass slider was investigated experimentally at a constant stator velocity of 1.4 m/s (Fig. 13). The average slider speed decreases with increasing weight per unit area of the slider. As discussed previously, an increase in weight per unit area of the slider leads to a decrease of the levitation distance, and this weakens the perpendicular turbulent flow in the Y direction, thus greatly reducing the eddy viscosity μ_e. As a result, the driving force decreases despite the increase in the energy density of the sound field between the slider and the stator.

The effect of the roughness of the bottom surface of the brass slider on the average slider speed was investigated experimentally, and the results are shown in Fig. 14. It is seen that the roughness of the bottom surface of the slider has an effect on the average slider speed, and there exists an optimum roughness between 1 μm $<$ Rz $<$ 5 μm at which the slider speed has a maximum. This can be explained as follows. When the bottom surface of the slider is too rough, the acoustic streaming near the bottom surface

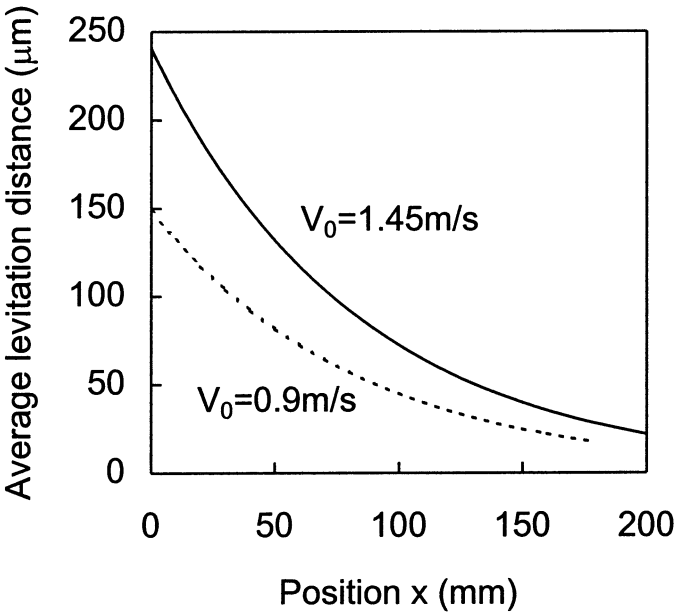

Fig. 15. Average levitation distance versus position for the glass slider at two stator vibration velocities.

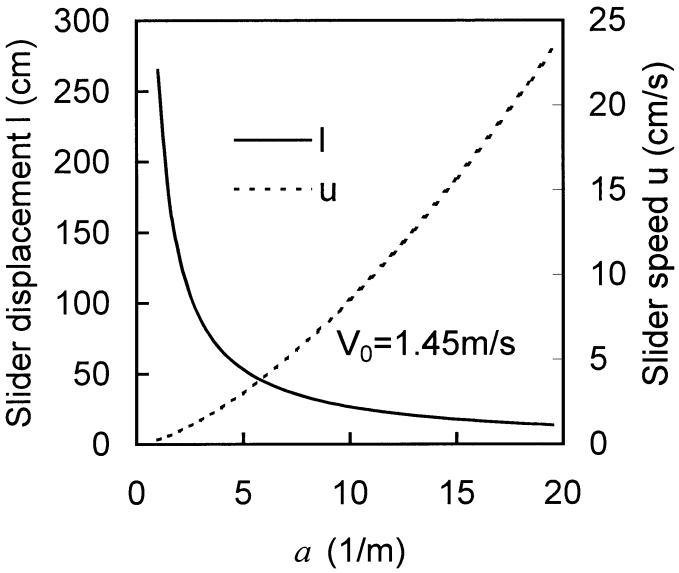

Fig. 16. Dependence of the displacement and average speed of the glass slider on the spatial attenuation factor of the stator vibration.

of the slider becomes weak because of the flow resistance. On the other hand, when the bottom surface of the slider is too smooth, the driving force becomes small because of the decrease of fluid impact in the horizontal direction.

The dependence of the average levitation distance h_a on position was calculated for the glass slider at two different V_0 (Fig. 15). The average levitation distance is proportional to the stator vibration amplitude and decreases with increasing x [(15), (18)].

The dependencies of the slider displacement and the average slider speed on the spatial attenuation factor of the stator vibration a was calculated for the glass slider at $V_0 = 1.45$ m/s (Fig. 16). The results show that when a increases (i.e., when the gradient of the stator vibration amplitude increases), the slider displacement decreases, and the average slider speed increases. The decrease of the slider displacement is due to the decrease of stator vibration amplitude, and the increase of the average slider speed is due to the increase of the acoustic streaming on the bottom surface of the slider.

Assuming that the stator vibration amplitude at $x = 0$ is 2 μm, the average slider speed of the brass slider was calculated as a function of driving frequency (Fig. 17). It is observed that the average slider speed decreases as the driving frequency increases. At driving frequencies less than 10 kHz, the slider speed increases very rapidly with decreasing driving frequency. In practice, the driving frequency may be decreased by increasing the thickness of the vibration excitation part of the stator.

In addition, from (18) and (24), it can be shown that the slider displacement is independent of the driving frequency when the average wave number k_x is much larger than the spatial attenuation factor a.

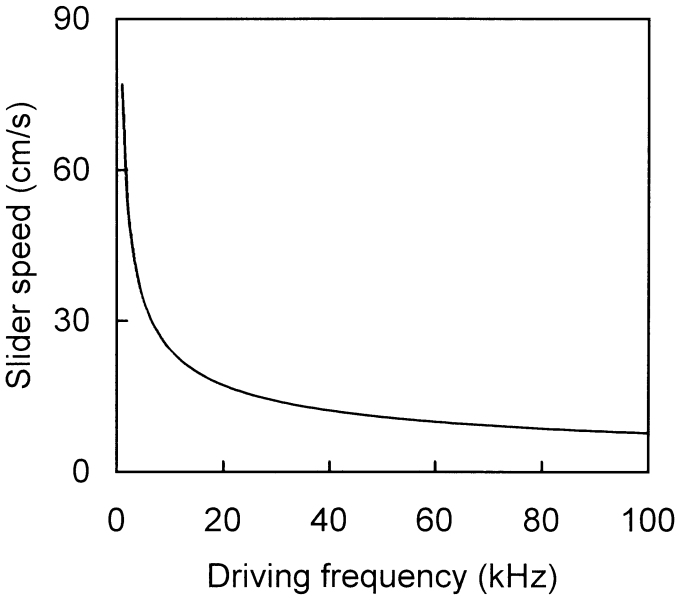

Fig. 17. Average speed of the brass slider versus driving frequency.

VII. Summary

In this paper, a standing wave-type noncontact linear ultrasonic motor is proposed. It uses a wedge-shaped stator to archive a gradient of the stator vibration amplitude to drive a slider. The upper surface of the stator is accurately adjusted to lie horizontally. At an input power of 2.5 W, a slider with a planar bottom surface and a weight per unit area of 7.4 mN/cm^2 can be transported 17 cm at an average speed of 10 cm/s. Furthermore, on the basis of the theories of near boundary acoustic streaming and turbulent flow, a theoretical model has been developed for the analysis of the characteristics of the motor. The model gives results that compare well with experimental data.

It is found that increasing the amplitude of the stator vibration displacement, decreasing the gradient of the stator vibration velocity, and decreasing the weight per unit area of the slider all increase the slider displacement. It is also found that increasing the amplitude and gradient of the stator vibration velocity, decreasing the weight per unit area of the slider, and decreasing the driving frequency all increase the slider speed. There is an optimum roughness of the bottom surface of the slider at which the slider speed has a maximum.

References

[1] M. Moroney, R. M. White, and R. T. Howe, "Ultrasonic micromotors," in *Proc. IEEE Ultrason. Symp.*, pp. 745–748, 1989.

[2] K. Nakamura, T. Ito, M. Kurozawa, and S. Ueha, "A trail construction of an ultrasonic motor with fluid coupling," *Jpn. J. Appl. Phys.*, vol. 29, pp. 160–161, 1990.

[3] Y. Yamayoshi and S. Hirose, "Ultrasonic motor not using mechanical friction force," *Int. J. Appl. Electromag. Mater.*, vol. 3, pp. 179–182, 1992.

[4] J. H. Hu, T. Yamazaki, K. Nakamura, and S. Ueha, "Analyses of an ultrasonic motor driving fluid directly," *Jpn. J. Appl. Phys.*, vol. 34, pp. 2702–2706, 1995.

[5] J. H. Hu, K. Nakamura, and S. Ueha, "Optimum operation conditions of an ultrasonic motor driving fluid directly," *Jpn. J. Appl. Phys.*, vol. 35, pp. 3289–3294, 1996.

[6] T. Yamazaki, J. H. Hu, K. Nakamura, and S. Ueha, "Trail construction of a noncontact ultrasonic motor with an ultrasonically levitated rotor," *Jpn. J. Appl. Phys.*, vol. 35, pp. 3286–3288, 1996.

[7] K. Nakamura, M. Maruyama, and S. Ueha, "A new ultrasonic motor using electro-rheological fluid and torsional vibration," *Ultrasonics*, vol. 34, pp. 261–264, 1996.

[8] J. H. Hu, K. Nakamura, and S. Ueha, "Characteristics of a noncontact ultrasonic motor using acoustic levitation," in *Proc. IEEE Ultrason. Symp.*, pp. 373–376, 1996.

[9] ——, "A noncontact ultrasonic motor with the rotor levitated by axial acoustic viscous force," *Trans. Inst. Electron. Inf. Commun. Eng. A*, vol. J80-A, no. 10, pp. 1705–1710, 1997. (in Japanese.)

[10] ——, "An analysis of a noncontact ultrasonic motor with an ultrasonically levitated rotor," *Ultrasonics*, vol. 35, pp. 459–467, 1997.

[11] ——, "A noncontact ultrasonic motor with the rotor levitated by axial acoustic viscous force," in *Proc. Ultrason. World Congress*, pp. 434–435, 1997.

[12] T. Zhou, G. Chen, D. Zang, S. Chen, and S. Dong, "The linear stepper motors with electrorheological fluid piezoelectric shear elements," in *Proc. Ultrason. World Congress*, pp. 436–437, 1997.

[13] Y. Hashimoto, Y. Koike, and S. Ueha, "Noncontact suspending and transporting planar objects by using acoustic levitation," *Trans. IEE Jpn.*, vol. 117-D, pp. 1406–1707, 1997.

[14] ——, "Magnification of transportation range using noncontact acoustic levitation by connecting vibration plates," *Jpn. J. Appl. Phys.*, vol. 36, pp. 3140–3145, 1997.

[15] ——, "Transporting objects without contact using flexural traveling wave," *J. Acoust. Soc. Jpn.*, vol. 103, pp. 3230–3233, 1998.

[16] J. H. Hu, "A study on noncontact high speed ultrasonic motors," Ph.D. dissertation, Tokyo Institute of Technology, 1997. (in Japanese.)

[17] J. Lighthill, *Waves in Fluid*. Cambridge: Cambridge University Press, 1978.

[18] M. M. Stanisic, *The Mathematical Theory of Turbulence*. New York: Springer-Verlag, 1988.

[19] S. Ueha, Y. Hashimoto, and Y. Koike, "Ultrasonic actuators using near field acoustic levitation," in *Proc. IEEE Ultrason. Symp.*, pp. 661–666, 1998.

[20] W. L. Nyborg, "Acoustic streaming near a boundary," *J. Acoust. Soc. Amer.*, vol. 30, pp. 329–339, 1958.

[21] C. P. Lee and T. G. Wang, "Near-boundary streaming around a small sphere due to two orthogonal standing waves," *J. Acoust. Soc. Amer.*, vol. 85, pp. 1081–1088, 1989.

[22] A. D. Pierce, *Acoustics*. New York: McGraw-Hill Book Company, 1981.

Junhui Hu (S'95–A'97) was born in China in August 1965. He received B.S. and M.S. degrees in electrical engineering from Zhejiang University, China and the Ph.D. degree from Tokyo Institute of Technology, Japan in 1986, 1989, and 1997, respectively. He was a research associate at the Department of Electrical Engineering, Zhejiang University from September 1989 to July 1991 and was a research engineer at R&D Center of Tokin Corporation, Japan from November 1997 to February 1999. Since March 1999, he has been a postdoctoral research fellow at the Center for Smart Materials, Department of Applied Physics, the Hong Kong Polytechnic University, Hong Kong. His present research includes ultrasonic motors, piezoelectric transformers, and other elastic wave functional devices.

Dr. Hu won the Paper Prize from the Institute of Electronics, Information and Communication Engineers (Japan) in 1998 and is the author and co-author of 15 disclosed patents on piezoelectric transformers. He is a member of IEEE-UFFC and the Acoustic Society of Japan.

Guorong Li received the B.S. degree in applied physics from Tongji University in 1985 and the M.S. degree in semiconductor and devices from Shanghai Institute of Technical Physics (SITP), Chinese Academy of Science (CAS), in 1988. From 1988 to 1992, he entered the joint Ph.D. course of SITP and material science and engineering of Yamagata University, Japan. He studied from October 1989 to March 1992 in Japan and received the Ph.D degree from SITP in 1992.

From 1992 to 1995, he was an assistant professor in polymer science and engineering, Shanghai Institute of Organic Chemistry, CAS. Since 1995, he has been an associate professor in functional organic ceramics, Shanghai Institute of Ceramics, CAS.

Since 1999, he has been working on the piezoelectric ultrasonic motors and transformers in applied physics, Hong Kong Polyuniversity, China. He received the excellent Young Scientist award in Shanghai, CAS, in 1997.

Helen Lai Wah Chan was born in Hong Kong in 1948. She received the B.Sc. and M. Phil. degrees in physics from the Chinese University of Hong Kong in 1970 and 1974, respectively, and the Ph. D. degree from Macquarie University, Australia, in 1987. Dr. Chan worked as a research scientist at CSIRO Division of Applied Physics in Sydney, N.S.W., Australia for four years. She was responsible for setting up the standards for medical ultrasound in Australia. She then worked at GEC-Marconi Pty. Australia for one year as a senior acoustic designer before returning to Hong Kong in 1992.

She is currently a professor of applied physics at the Hong Kong Polytechnic University.

Chung Loong Choy was born in Malaysia in 1938. He received the Ph.D. degree in physics from Rensselaer Polytechnic Institute in 1968 and then worked as a research associate for one year at Cornell University. He was a visiting scientist at the University of Leeds, the University of Massachusetts, and Sydney University in 1974, 1981, and 1993, respectively. His current research interest is on ferroelectric materials and their applications.

Dr. Choy is presently Chair Professor and Head of the Department of Applied Physics at the Hong Kong Polytechnic University.